COMPDYN 2013
4th ECCOMAS Thematic Conference on
Computational Methods in Structural Dynamics and Earthquake Engineering
M. Papadrakakis, V. Papadopoulos, V. Plevris (eds.)
Kos Island, Greece, 12–14 June 2013

PERFECTLY MATCHED LAYER (PML) FOR TRANSIENT WAVE PROPAGATION IN A MOVING FRAME OF REFERENCE

Stine S. Madsen[1], **Steen Krenk**[2] **and Ole Hededal**[1]

[1]Department of Civil Engineering / [2]Department of Mechanical Engineering
Technical University of Denmark
DK-2800 Kgs. Lyngby, Denmark
e-mail: sskk@byg.dtu.dk / sk@mek.dtu.dk / olh@byg.dtu.dk

Keywords: Absorbing boundaries, PML, Finite element, Moving load, Wave propagation.

Abstract. *In relation to the development of a Rolling Wheel Deflectometer (RWD), which is a non-destructive testing device for measuring pavement deflections, a finite element model for obtaining the soil/pavement response is developed. Absorbing boundary conditions are necessary in order to prevent reflections of the waves propagating through the soil due to the dynamic loading. The Perfectly Matched Layer (PML) has proven to be highly efficient when solving transient wave propagation problems in a fixed mesh. However, since the RWD is operating at traffic speeds, the load is moving with high speed and a formulation in a moving mesh is therefore more convenient. In this paper, a formulation of the PML is developed in the moving frame of reference. Numerical results are presented for a single layer and a double layer half space, respectively, subjected to a moving load of different velocities.*

1 INTRODUCTION

The Rolling Wheel Deflectometer (RWD) is a non-destructive testing device operating at traffic speed for measuring pavement deflections. The RWD is equipped with a heavy load on the rear-most axle under which the pavement deflections are measured. A 2D finite element model is developed in order to obtain the soil/pavement response from a transient dynamic load simulating the heavy load from the RWD. Absorbing boundary conditions are necessary in order to prevent reflections of the waves propagating through the soils due to the dynamic loading. As the load is moving at high speed, the use of a fixed mesh will require a very large computational domain in order to capture the response under the moving load before it leaves the domain. This can be quite costly and limit the analysis to a rather short time interval. A formulation in the moving frame of reference is therefore more convenient.

A local transmitting boundary condition formulated in convective coordinates developed by Krenk et al. [1, 2] has been used in transient vibration analysis of railway-ground system under fast moving loads [3]. The formulation is simple and computationally fast, essentially being equivalent to an oriented spring-damper configuration at the boundary nodes, based on planar waves with a single point of origin. In the moving coordinate system, the directions of propagation of P- and S-waves are modified to account for the translation of the frame of reference.

The radiation formulation can be made more general and robust by extending it to non-local form by using an additional attenuation layer around the computational domain, in the form of a Perfectly Matched Layer (PML) first proposed by Berenger [4] to electromagnetic waves. Later PML was formulated for the elastic wave equation in e.g. [5, 6, 7]. However, in this approach the solution for the displacements is dependent on computation of the strains in each time step. A simpler procedure, depending only on the displacements, using an artificially anisotropic material description of the PML layer, was recently proposed in [8]. Compared to the spring-damper configuration, the additional layer contains more information about propagation directions and has proven to be highly efficient when solving transient vibration problems in a stationary frame of reference [8]. The PML has not yet been formulated in the moving frame of reference.

In this paper, a formulation of the PML is developed in translating coordinates based on the PML formulation in [8]. Numerical results are presented for a half-space subjected to a moving load of different velocities and a half-space of multiple layers.

2 PERFECTLY MATCHED LAYER

The standard PML formulation of [8], valid for transient wave propagation in a stationary mesh, is generalized to a moving mesh. The key concept of the PML is a coordinate transformation in which the spatial variables are mapped onto complex space by a so-called complex stretching function. The mapping replaces propagating waves with exponentially decaying waves as the propagating waves passes the PML interface. The general equation of motion is written as

$$\nabla \boldsymbol{\sigma} + \boldsymbol{p} = \rho \ddot{\boldsymbol{u}} \tag{1}$$

$$\sigma = \boldsymbol{C}\boldsymbol{\varepsilon} = \boldsymbol{C}\nabla \boldsymbol{u} \tag{2}$$

where $\boldsymbol{u} = [u_1, u_2]^T$ is the displacement vector, $\boldsymbol{p} = [p_1, p_2]^T$ is the load vector, and $\dot{(\,)}$ denotes temporal differentiation. $\boldsymbol{\sigma}$ is the stress tensor defined by

$$\boldsymbol{\sigma} = \begin{bmatrix} \sigma_{11} & \sigma_{12} \\ \sigma_{21} & \sigma_{22} \end{bmatrix} \tag{3}$$

In the absorbing layer the original coordinate variables x_i, $(i = 1, 2)$ are replaced with the complex stretched coordinate variables $\tilde{x}_i$, defined by

$$\tilde{x_i} = \int_0^{x_i} s_i(\hat{x}_i, \omega) \mathrm{d}\hat{x}_i, \quad i = 1, 2 \tag{4}$$

where ω is the angular frequency and s_i are the stretched coordinate functions proposed in [9]

$$\frac{\partial \tilde{x}_i}{\partial x_j} = s_i(x_i, \omega) = 1 + \frac{\beta_i(x_i)}{i\omega}, \quad i = 1, 2 \tag{5}$$

where i denotes the imaginary unit and $\beta \geq 0$ is a real function which controls the attenuation of the wave propagation.

Applying the stretched coordinates to the equation of motion (1) in a frequency representation yields

$$\nabla_s \boldsymbol{\sigma} + \boldsymbol{p} = -\omega^2 \rho \, \boldsymbol{u} \tag{6}$$

where $u(t) = U(\omega)e^{-i\omega t}$, $\nabla_s = (\partial/\partial\tilde{x}_1, \partial/\partial\tilde{x}_2)^T$, and $\frac{\partial}{\partial \tilde{x}_i} = \frac{1}{s_i}\frac{\partial}{\partial x_i}$. Because the equations in the complex stretched coordinates are on the same form as those in the non-stretched coordinates, waves are passing through the PML interface without causing any reflections [10].

The introduction of the stretched coordinates yields an anisotropic formulation of the equation of motion, expressed by ∇_s. To keep the expressions of the divergence and the gradient in non-stretched coordinates, the anisotropy is moved to the material description by a modification of the constitutive relation, allowing for the use of the same kinematics in the computational domain and PML domain. Equation (6) is multiplied with the product $s_1 s_2$ and a new set of stress variables is introduced, defined in tensor form as

$$\tilde{\boldsymbol{\sigma}} = s_1 s_2 \begin{bmatrix} s_1^{-1} & 0 \\ 0 & s_2^{-1} \end{bmatrix} \boldsymbol{\sigma} = s_1 s_2 \boldsymbol{\Lambda} \boldsymbol{\sigma} \tag{7}$$

By substitution of equation (7) into (2) and modifying the constitutive relation, the equation of motion with the new stress variables can be written in non-stretched coordinates as

$$\nabla \tilde{\boldsymbol{\sigma}} + \boldsymbol{p} = -\rho\omega^2 s_1 s_2 \boldsymbol{u} \tag{8}$$

$$\tilde{\boldsymbol{\sigma}} = \tilde{\boldsymbol{C}} \nabla \boldsymbol{u} \tag{9}$$

where the constitutive relation is modified to

$$\tilde{C}_{ijkl} = \frac{s_1 s_2}{s_i s_k} C_{ijkl} \quad , \quad i, j, k, l = 1, 2 \tag{10}$$

with no summation over indices i and k. This formulation leads to an artificial anisotropic material description since $\tilde{C}_{1111} \neq \tilde{C}_{2222}$.

For a general FE-implementation, equation (9) is formulated in Voigt notation, and the constitutive law then reads

$$\begin{bmatrix} \tilde{\sigma}_{11} \\ \tilde{\sigma}_{22} \\ \frac{1}{2}\left(\tilde{\sigma}_{21}+\tilde{\sigma}_{12}\right) \\ \frac{1}{2}\left(\tilde{\sigma}_{21}-\tilde{\sigma}_{12}\right) \end{bmatrix} = \begin{bmatrix} \tilde{C}_{11} & C_{12} & & \\ C_{21} & \tilde{C}_{22} & & \\ & & \tilde{C}'_{66} & \tilde{C}''_{66} \\ & & \tilde{C}''_{66} & \tilde{C}'''_{66} \end{bmatrix} \begin{bmatrix} \frac{\partial}{\partial x_1} & 0 \\ 0 & \frac{\partial}{\partial x_2} \\ \frac{\partial}{\partial x_2} & \frac{\partial}{\partial x_1} \\ \frac{\partial}{\partial x_2} & -\frac{\partial}{\partial x_1} \end{bmatrix} \begin{bmatrix} u_1 \\ u_2 \end{bmatrix} \tag{11}$$

where $\tilde{C}_{11} = s_2 C_{11}/s_1$, $\tilde{C}_{22} = s_1 C_{22}/s_2$, and the shear-related parameters are given by

$$\tilde{C}'_{66} = \frac{C_{66}}{4}\left(\frac{s_1}{s_2}+\frac{s_2}{s_1}+2\right) \tag{12}$$

$$\tilde{C}''_{66} = \frac{C_{66}}{4}\left(\frac{s_1}{s_2}-\frac{s_2}{s_1}\right) \tag{13}$$

$$\tilde{C}'''_{66} = \frac{C_{66}}{4}\left(\frac{s_1}{s_2}+\frac{s_2}{s_1}-2\right) \tag{14}$$

Equation (11) can be written in the compact form $\tilde{\boldsymbol{\sigma}}_v = \tilde{\boldsymbol{C}}\boldsymbol{\partial}\boldsymbol{u}$ where subscript v indicates Voigt notation and the strain-displacement operator is

$$\boldsymbol{\partial} = \begin{bmatrix} \frac{\partial}{\partial x_1} & 0 \\ 0 & \frac{\partial}{\partial x_2} \\ \frac{\partial}{\partial x_2} & \frac{\partial}{\partial x_1} \\ \frac{\partial}{\partial x_2} & -\frac{\partial}{\partial x_1} \end{bmatrix} \tag{15}$$

The derived equations cover both the computational domain and the PML regions since $\beta_i = 0$ in the computational domain which leaves $s_i = 1$, resulting in the general formulation of the wave equation.

The frequency-dependent equation of motion (8) is transformed into the time domain using the inverse Fourier transform [11], yielding

$$\nabla\tilde{\boldsymbol{\sigma}}_v + \boldsymbol{p} = \rho\,\mathcal{D}_0(t)\boldsymbol{u} \tag{16}$$

$$\tilde{\boldsymbol{\sigma}}_v = \tilde{\boldsymbol{C}}\partial\boldsymbol{u} \tag{17}$$

where the operator $\mathcal{D}_0(t)$ is the inverse Fourier transform of $-\omega^2 s_1 s_2$, given by

$$\mathcal{D}_0(t) = \frac{d^2}{dt^2} + (\beta_1+\beta_2)\frac{d}{dt} + \beta_1\beta_2 \tag{18}$$

The modified constitutive relation is given by

$$\tilde{\boldsymbol{C}} = \boldsymbol{C} + \mathcal{F}_1(t)\boldsymbol{C}_1 + \mathcal{F}_2(t)\boldsymbol{C}_2 \tag{19}$$

where $\boldsymbol{C}$ is the non-stretched constitutive matrix and $\boldsymbol{C}_1$, $\boldsymbol{C}_2$ represent two stretched parts of the constitutive matrix, see the appendix. The operators $\mathcal{F}_1(t)$ and $\mathcal{F}_2(t)$ are the inverse Fourier transform of s_1/s_2 and s_2/s_1, respectively, given by

$$\mathcal{F}_1(t) = (\beta_1-\beta_2)e^{-\beta_1 t}, \quad t \geq 0 \tag{20}$$

$$\mathcal{F}_2(t) = (\beta_2-\beta_1)e^{-\beta_2 t}, \quad t \geq 0 \tag{21}$$

2.1 Convective coordinates

The formulation in a fixed coordinate system X_i, is transfered into a moving coordinate system x_i, via the relation [1]

$$x_i = X_i - Vt \tag{22}$$

where V is the velocity of the vehicle. The equilibrium equations are expressed in the moving coordinate system by introducing the partial differentiation operators

$$\left.\frac{\partial}{\partial X}\right|_t = \left.\frac{\partial}{\partial x}\right|_t , \qquad \left.\frac{\partial}{\partial t}\right|_X = \left.\frac{\partial}{\partial t}\right|_x - V\frac{\partial}{\partial x} \tag{23}$$

following from the relation (22) between the two coordinate systems.

Substitution of the operators into Equation (16) modifies the equilibrium equations to

$$\nabla\tilde{\boldsymbol{\sigma}}_v + \boldsymbol{p} = \rho\,\tilde{\mathcal{D}}_0\boldsymbol{u} \tag{24}$$

$$\tilde{\boldsymbol{\sigma}}_v = \tilde{\boldsymbol{C}}\partial\boldsymbol{u} \tag{25}$$

with the convected operator

$$\tilde{\mathcal{D}}_0 = \left(\frac{\partial}{\partial t} - V\frac{\partial}{\partial x}\right)^2 + (\beta_1+\beta_2)\left(\frac{d}{dt} - V\frac{d}{dx}\right) + \beta_1\beta_2 \tag{26}$$

The convolution equations related to (17) are not directly dependent on time, hence they remain unchanged. The transformation from fixed to moving coordinates only modifies the ordinary equation of motion, making it simple to implement in the PML formulation.

2.2 Finite element implementation

The principle of virtual work is used to obtain the weak formulation of the equation of motion (24), yielding

$$\int_\Omega (\delta\boldsymbol{u})^T\rho\,\tilde{\mathcal{D}}_0\boldsymbol{u}d\Omega + \int_\Omega (\partial\delta\boldsymbol{u})^T\tilde{\boldsymbol{\sigma}}_v d\Omega - \int_\Omega (\delta\boldsymbol{u})^T\boldsymbol{p}d\Omega - \int_\Gamma (\delta\boldsymbol{u})^T\boldsymbol{T}d\Gamma = 0 \tag{27}$$

The spatial variation of the actual and the virtual displacement fields are represented by shape functions as

$$\boldsymbol{u}(x,t) = \boldsymbol{N}(x)\boldsymbol{d}(t) \tag{28}$$

$$\widehat{\boldsymbol{u}}(x,t) = \widehat{\boldsymbol{N}}(x)\widehat{\boldsymbol{d}}(t) \tag{29}$$

with the shape functions $\boldsymbol{N}$ on the form

$$\boldsymbol{N} = \begin{bmatrix} N_1 & 0 & N_2 & 0 & \cdots & N_n & 0 \\ 0 & N_1 & 0 & N_2 & \cdots & 0 & N_n \end{bmatrix} \tag{30}$$

and $\widehat{\boldsymbol{N}}$ in a similar form. Separating the convolution terms in the operators $\mathcal{F}_1(t)$ and $\mathcal{F}_2(t)$ the following set of ordinary differential equations is obtained

$$\boldsymbol{M}\ddot{\boldsymbol{d}} + \boldsymbol{Z}\dot{\boldsymbol{d}} + \boldsymbol{K}\boldsymbol{d} + \tilde{\boldsymbol{g}} = \boldsymbol{f} \tag{31}$$

where $\boldsymbol{d}$ is the global displacement vector. $\boldsymbol{f}$ is the global force vector determined by

$$\boldsymbol{f}^e = \int_{\Omega^e} \boldsymbol{N}^T \boldsymbol{p} d\Omega \tag{32}$$

where only point loading on the free surface is assumed. The element mass, damping and stiffness matrices $\boldsymbol{M}^e$, $\boldsymbol{Z}^e$ and $\boldsymbol{K}^e$, are given by

$$\boldsymbol{M}^e = \int_{\Omega^e} \rho \widehat{\boldsymbol{N}}^T \boldsymbol{N} \mathrm{d}\Omega \tag{33}$$

$$\boldsymbol{Z}^e = \int_{\Omega^e} \left(\rho(\beta_1 + \beta_2) \widehat{\boldsymbol{N}}^T \boldsymbol{N} + \rho V \left(\widehat{\boldsymbol{N}}_x^T \boldsymbol{N} - \widehat{\boldsymbol{N}}^T \boldsymbol{N}_x \right) \right) \mathrm{d}\Omega \tag{34}$$

$$\boldsymbol{K}^e = \int_{\Omega^e} \left(\widehat{\boldsymbol{B}}^T \boldsymbol{C} \boldsymbol{B} + \rho \beta_1 \beta_2 \widehat{\boldsymbol{N}}^T \boldsymbol{N} \right) \mathrm{d}\Omega \tag{35}$$

$$+ \int_{\Omega^e} \left(-\rho V(\beta_1 + \beta_2) \widehat{\boldsymbol{N}}^T \boldsymbol{N}_x + V^2 \widehat{\boldsymbol{N}}_x^T \boldsymbol{N}_x \right) \mathrm{d}\Omega \tag{36}$$

where $\boldsymbol{B}$ denotes the strain-displacement matrix and $\boldsymbol{N}$ the shape functions with x-derivative $\boldsymbol{N}_x = \partial \boldsymbol{N} / \partial \boldsymbol{x}$. Assuming constant PML parameters inside each element the convolution vector $\tilde{\boldsymbol{g}}$ is given by

$$\tilde{\boldsymbol{g}}^e = \boldsymbol{K}_2^e \left(\mathcal{F}_1 * u(t) \right) + \boldsymbol{K}_1^e \left(\mathcal{F}_2 * u(t) \right) \tag{37}$$

where the element matrices $\boldsymbol{K}_1$ and $\boldsymbol{K}_2$ are given by

$$\boldsymbol{K}_p^e = - \int_{\Omega} \boldsymbol{B}^T \boldsymbol{C}_p \boldsymbol{B} \mathrm{d}\Omega \,, \quad p = 1, 2 \tag{38}$$

The convolution terms $\mathcal{F}_p * u(t)$ are defined on each element of the mesh and are discontinuous from one element to another since the PML parameters are assumed element-wise constant. The general appearance of the convolution term is

$$\mathcal{F}_p * u(t) = \int_0^t \mathcal{F}_p(\tau) u(t - \tau) d\tau = \int_0^t (\beta_p - \beta_{\bar{p}}) e^{-\beta_{\bar{p}} \tau} u(t - \tau) d\tau \tag{39}$$

with index $\bar{p}$ being the complement of p. When assuming $u(t)$ piece-wise constant in the time interval $[t_n,\ t_{n+1}]$, the solution can be reformulated to increment form via integration by parts, and the convolution integrals then only require information from the last time step.

The finite element equation system is solved for the displacements using bilinear elements with a Newmark-based time integration method, see e.g. [8].

3 NUMERICAL EXAMPLES

Two numerical examples are presented to demonstrate the absorbing properties of the suggested formulation in translating coordinates. The two examples involve a moving transient dynamic load traveling on the surface of a single layer half space and a double layer half-space, respectively, see Figure 1. The layers are indicated in Figure 1 as the areas Ω_1 and Ω_2 and the PML layer surrounds the computational domain indicated by a dashed line. The computational domain is 156m wide, corresponding to approximately two pressure wave lengths, and 78m deep. The material parameters of the two layers are listed in Table 1. The dynamic response is

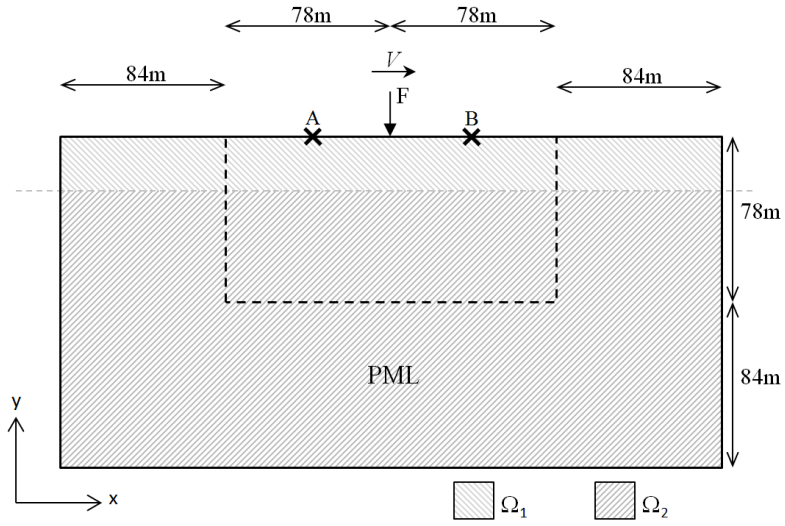

Figure 1: Illustration of numerical example. The observation points where the response is recorded is marked with two crosses. The interface between PML and the computational domain is indicated by a dashed line.

Table 1: Material parameters of the layered soil in Figure 1.

Material	E [MPa]	ν	ρ [kg/m^3]	c_p [m/s]	c_s [m/s]	c_r [m/s]
Ω_1	125	0.25	2000	273.9	158.1	145.5
Ω_2	250	0.25	2000	387.3	223.6	205.7

obtained from two observation points A and B placed on each side of the load at a distance of 39m corresponding to slightly more than one half pressure wave length. The load is defined as

$$F(x,t) = T(t)\delta(x - x^c) \tag{40}$$

where δ is the Dirac delta function and x^c is the location of the point source with temporal evolution $T(t)$ defined by

$$T(t) = \tau(1-\tau^2)^2, \quad -1 < \tau < 1 \tag{41}$$

where $\tau = 2t/T - 1$. The total duration of the pulse is $T = 0.2s$ and the dominant frequency of the pulse is $f = 1/T = 5Hz$. In the numerical examples, the maximum load is $F_{max} = 1$MN.

The spatial dependence of the PML parameter β_i in the x_i direction is chosen as in [8]

$$\beta_i = \beta_i^{max} \left(\frac{x_i^p}{d_i} \right)^{n_1+n_2} \tag{42}$$

in which x_i^p is measured from the interface to PML and d_i is the thickness of the PML layer. The coefficient β_i^{max} is given by [8]

$$\beta_i^{max} = -\frac{(1+n_1+n_2)c_p log_{10}(R_0)}{2d_i} \tag{43}$$

for $i = 1, 2$. Here R_0 is the theoretical reflection coefficient at normal incidence and c_p is the pressure wave velocity. In this example the following values for the parameters are chosen to: $R_0 = 10^{-8}$, $n_1 = 3$, $n_2 = 0$ and $d_i = 84$m corresponding to slightly more than two Rayleigh wave lengths.

3.1 Example 1: Single layer

In the single layer experiment the material parameters of the layers indicated in Figure 1 are equal, corresponding to material Ω_2 in Table 1. The element edge length is $\Delta x_1 = \Delta x_2 = 3.9$m corresponding to 20 elements per pressure wave length, and the time step is $\Delta t = 0.0071$s such that it meets the CFL condition defined by

$$\Delta t_c = \min\big[\Delta x_1, \Delta x_2\big]/c_p \tag{44}$$

The simulations run for 1.0 s, requiring 140 time steps. The load is traveling on the surface of the single layer half-space with the three different velocities $M = V/c_s = 0, 0.2, 0.4$. The responses are obtained at the two observation points A and B. The time evolutions are visualized in Figure 2 where the load signal is perfectly transported through the observation points without sending any reflections back from the boundaries. The pulse arrives at around 0.19s corresponding to the time of arrival for the Rayleigh wave, which is $39\,\mathrm{m}/205.7\,\mathrm{m/s} = 0.19\,\mathrm{s}$. Since the load is traveling from left to right the pulse delay increases with increasing velocity at point B while it decreases at point A. The response is seen to increase with velocity in front of the load, at point B, while it decreases behind the load, at point A.

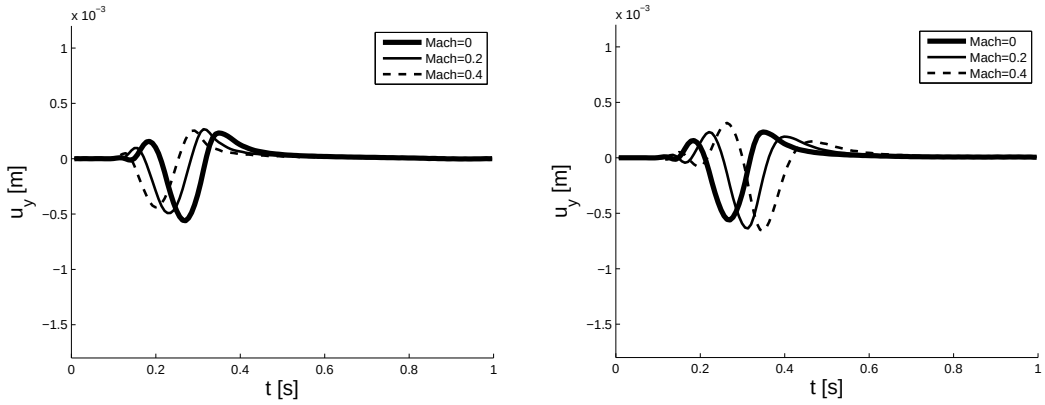

Figure 2: Single layer half-space: Vertical displacement response at two observation points A (left) and B (right) with velocity $M = 0.0, 0.2, 0.4$.

3.2 Example 2: Two layers

The material properties of the two layers are given by Ω_1 and Ω_2 as indicated in Figure 1. The top layer indicated by Ω_1 has a thickness of 7.8m and it is half as stiff as the bottom layer. Both the computational domain and the PML domain experience a change in material parameters at the interface between the two layers. The same element edge length and time step is used as in Example 1, where the time step $\Delta_t = 0.0071$ is determined based on the thicker bottom layer to ensure observance of the CFL condition in the entire domain. The time evolutions of the pulse obtained from observation point A and B are illustrated in Figure 3. The introduction of a softer surface layer causes a general increase in the response for all three velocities. It also becomes more clear that the response increases with velocity at point B, while it decreases at point A. However, in spite of the sudden material change at the interface between the top and bottom layers, the PML works very well for all three velocities. Only a slight disturbance is observed after the wave has passed. This may be avoided by adjusting the parameter β or by increasing the thickness of the PML layer.

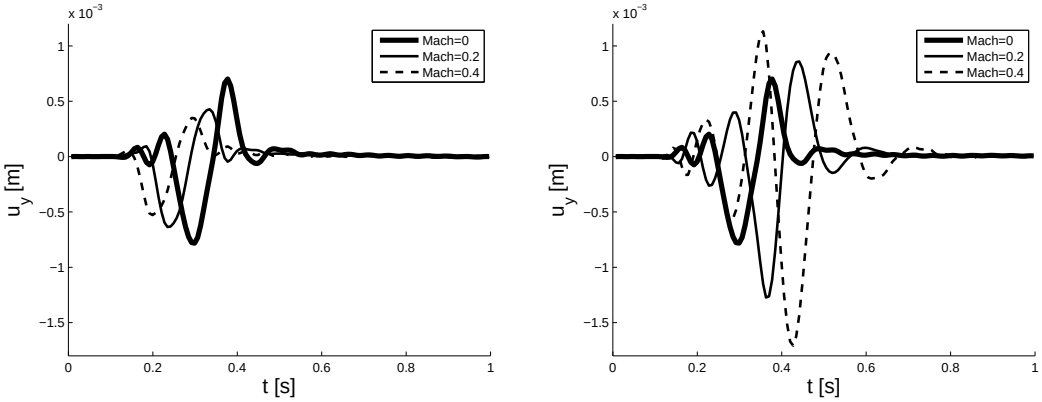

Figure 3: Two-layer half-space: Vertical displacement response at two observation points A (left) and B (right) with velocity $M = 0.0, 0.2, 0.4$.

4 CONCLUSION

The PML formulation for transient wave propagation has been generalized to a moving frame of reference. The transformation from fixed to moving coordinates only modifies the ordinary differential equation of motion and is therefore simple to implement in the PML equations. The applicability of the formulation was successfully tested on two numerical examples; a single layer and a double layer half-space, respectively.

REFERENCES

[1] S. Krenk, L. Kellezi, S. R. K. Nielsen, P. H. Kirkegaard, Finite elements and transmitting boundary conditions for moving loads, in: EURODYN'99, 4th European Conference on Structural Dynamics; Prague, June 7-10, 1999, Balkema, Rotterdam, 1999, pp. 447–452.

[2] S. Krenk, P. Kirkegaard, Local tensor radiation conditions for elastic waves, Journal of Sound and Vibration 247 (5) (2001) 875–896.

[3] W. Zhai, E. Song, Three dimensional fem of moving coordinates for the analysis of transient vibrations due to moving loads, Computers and Geotechnics 37 (1-2) (2010) 164–174.

[4] J.-P. Berenger, A perfectly matched layer for the absorption of electromagnetic waves, Journal of Computational Physics 114 (2) (1994) 185–200.

[5] U. Basu, A. Chopra, Perfectly matched layers for time-harmonic elastodynamics of unbounded domains: theory and finite-element implementation, Computer Methods in Applied Mechanics and Engineering 192 (11-12) (2003) 1337–1375.

[6] U. Basu, A. Chopra, Perfectly matched layers for transient elastodynamics of unbounded domains, International Journal for Numerical Methods in Engineering 59 (8) (2004) 1039–1074.

[7] U. Basu, Explicit finite element perfectly matched layer for transient three-dimensional elastic waves, International Journal for Numerical Methods in Engineering 77 (2) (2009) 151–176.

[8] R. Matzen, An efficient finite element time-domain formulation for the elastic second-order wave equation: A non-split complex frequency shifted convolutional PML, International Journal for Numerical Methods in Engineering 88 (10) (2011) 951–973.

[9] M. Kuzuoglu, R. Mittra, Frequency dependence of the constitutive parameters of causal perfectly matched anisotropic absorbers, IEEE Microwave and Guided Wave Letters 6 (12) (1996) 447–449.

[10] Y. Zheng, X. Huang, Anisotropic perfectly matched layers for elastic waves in cartesian and curvilinear coordinates anisotropic PML for elastic waves (1997) 1–18.

[11] R. N. Bracewell, The Fourier transform and its applications, McGraw-Hill, Boston, MA, 2000.

A CONSTITUTIVE MATRICES

The entries in the modified constitutive matrix $\tilde{\boldsymbol{C}}$ related to s_1/s_2 and s_2/s_1 are represented in the two stretched constitutive matrices $\boldsymbol{C}_1$ and $\boldsymbol{C}_2$, given by

$$\boldsymbol{C}_1 = \begin{bmatrix} 0 & 0 & 0 & 0 \\ 0 & \lambda+2\mu & 0 & 0 \\ 0 & 0 & \mu/4 & \mu/4 \\ 0 & 0 & \mu/4 & \mu/4 \end{bmatrix} \tag{A.1}$$

$$\boldsymbol{C}_2 = \begin{bmatrix} \lambda+2\mu & 0 & 0 & 0 \\ 0 & 0 & 0 & 0 \\ 0 & 0 & \mu/4 & -\mu/4 \\ 0 & 0 & -\mu/4 & \mu/4 \end{bmatrix} \tag{A.2}$$

The non-stretched constitutive matrix $\boldsymbol{C}$ is given by

$$\boldsymbol{C} = \begin{bmatrix} \lambda+2\mu & \lambda & 0 & 0 \\ \lambda & \lambda+2\mu & 0 & 0 \\ 0 & 0 & \mu & \mu \\ 0 & 0 & \mu & \mu \end{bmatrix} \tag{A.3}$$

in which μ, λ are the Lamé constants.